A discrete water exit pathway in the membrane protein cytochrome *c* oxidase

Bryan Schmidt*†, John McCracken†, and Shelagh Ferguson-Miller*‡

Departments of *Biochemistry and †Chemistry, Michigan State University, East Lansing, MI 48824

Edited by Harry B. Gray, California Institute of Technology, Pasadena, CA, and approved October 27, 2003 (received for review May 28, 2003)

By using the non-redox-active Mg^{2+}/Mn^{2+} site of cytochrome *c* oxidase as a probe, water access from the outside of the enzyme and water escape from the buried active site were studied. Water movement was time-resolved by monitoring the magnetic interaction of the oxygen isotope ^{17}O with the Mn^{2+} by using a rapid freeze-quench–electron spin echo envelope modulation technique. Rapid (msec) access of water from the bulk phase to the Mn^{2+} was demonstrated by mixing cytochrome *c* oxidase with $H_2{}^{17}O$. To determine whether a channel involving the Mn^{2+} was used for water exit from the active site, samples incubated in $^{17}O_2$ were allowed to turn over approximately five times before freezing. The ^{17}O, now in the form of $H_2{}^{17}O$, was detected at the Mn^{2+}. The significant broadening of the Mn^{2+} signal after the limited number of turnovers strongly suggests that the water exits the protein by means of one discrete pathway, not by random diffusion.

Cytochrome *c* oxidase (CcO) is an intrinsic membrane protein that functions as the terminal enzyme of the respiratory electron transport chain. CcO transfers electrons from cytochrome *c* to dioxygen, which is reduced to water, through four redox-active metal centers: a dinuclear copper site, Cu_A; a heme *a*; and the binuclear active site, consisting of another heme, heme a_3, and copper, Cu_B (1). In addition to the four protons per O_2 taken up from the inner side of the membrane for the oxygen chemistry, an additional four protons are pumped across the membrane (2). The net result is the production of an electrochemical gradient that is used to drive a variety of processes, most notably ATP synthesis. Site-specific mutagenesis and high-resolution crystal structures of bacterial and mammalian CcO have defined two proton intake pathways (3–5), but the route for exit of pumped protons is not yet clear (6–9).

Besides the redox-active metal centers, in all eukaryotic CcO the region above the hemes contains a non-redox-active metal site containing a Mg^{2+} (Fig. 1). This region contains an intricately hydrogen-bonded network of water with suggestions of paths to the surface. The reason for this non-redox-active metal at a site 12 Å from the active site is puzzling, and its total conservation in eukaryotes suggests that it serves an important role.

In addition to proton and electron movement, water is generated at rates as high as 1,000 sec^{-1}. Spatial constraints provide a driving force for expulsion of the product water from the active site. Although there have been a few proposals for water exit channels (10–13), the crystal structures do not show any clear routes from the active site (Fig. 2). Indeed, it can be argued that no channel is necessary, because water has been shown to rapidly exchange within proteins (14, 15). However, the function of CcO as a proton pump suggests that access of water to random sites within the protein is not likely. CcO requires the controlled movement of electrons and protons, and therefore water, because the latter can serve as a pathway for the protons, preferentially short-circuiting the pump (16, 17).

Previous electron spin echo envelope modulation (ESEEM) studies of ^2H_2O exchange at the buried Mg^{2+} site, substituted with Mn^{2+}, indicated rapid access of deuterium to the metal (18) but could not distinguish whether it was $^2H^+$ or ^2H_2O that was reaching the site. The studies reported here, using $H_2{}^{17}O$ and $^{17}O_2$, make that distinction, showing that water itself can access the Mg^{2+}/Mn^{2+} site from the outside bulk water and from the interior active site.

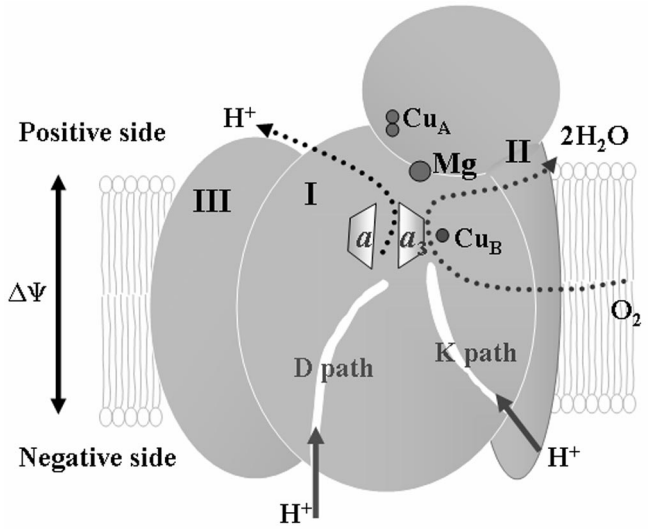

Fig. 1. Overall structure of CcO. CcO is composed of three core subunits. Subunit I contains the binuclear active site of heme *a*–Cu_B and heme *a*. Subunit II contains the dinuclear Cu_A site, the initial electron acceptor. Subunit III does not contain any redox-active metal cofactors. The Mg^{2+} site is situated between subunits I and II and above the binuclear active site. The D and K paths are proton uptake pathways named for a conserved aspartate and lysine, respectively.

Materials and Methods

Protein Production and Purification. To obtain Mn^{2+} enrichment at the Mg^{2+} site in the protein, the YZ300 strain of *Rhodobacter sphaeroides* (19) was grown on high-Mn^{2+} medium to ensure preferential incorporation of Mn^{2+} over Mg^{2+} (20). The protein was purified by Ni^{2+}–nitrilotriacetic acid affinity chromatography (21) and further purified by DEAE ion-exchange chromatography. For all experiments, the CcO was maintained in buffer containing 50 mM KH_2PO_4–KOH, 0.1 mM EDTA, and 0.1% lauryl maltoside at pH 7.4.

Rapid-Mix Freeze–Quench Exchange. Rapid kinetics were obtained by using an Update Instruments (Madison, WI) System 1000 Chemical/Freeze–Quench apparatus (model 715 Ram Controller and model 1019 Syringe Ram) with modified funnel and syringes (18). For experiments in which there was turnover of the

This paper was submitted directly (Track II) to the PNAS office.

Abbreviations: CcO, cytochrome *c* oxidase; ESEEM, electron spin echo envelope modulation; RFQ, rapid freeze–quench.

‡To whom correspondence should be addressed. E-mail: fergus20@pilot.msu.edu.

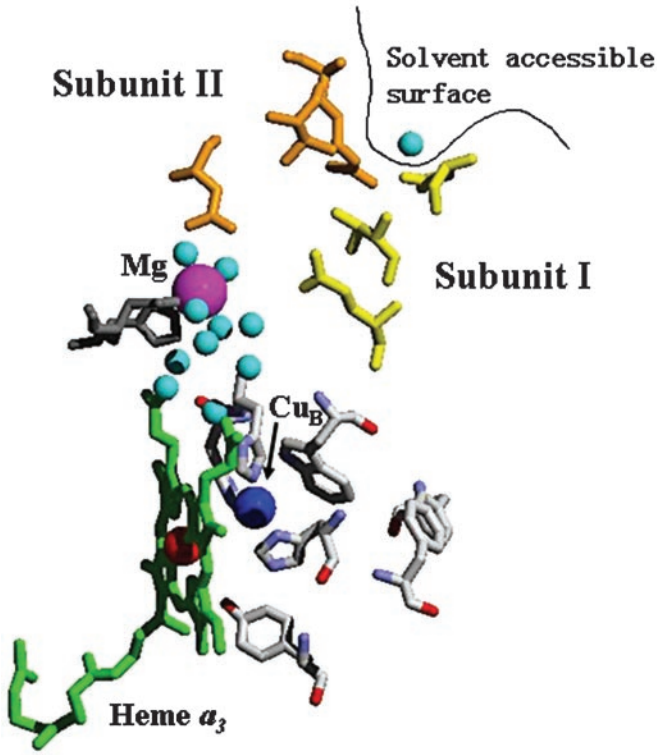

Fig. 2. Active site and possible exit pathway. The binuclear active site (heme a_3 in green and Cu_B in blue) is 13 Å from the Mn^{2+} (magenta sphere) but is hydrophobically isolated. Once water from the active site reaches the Mn^{2+}, it then has several possible routes to the bulk, including a proposed channel (18) that contains residues along the interface of subunit I (colored yellow) and subunit II (colored orange). The distance from the Mn^{2+} to the solvent-accessible surface (black line) is 13 Å. The crystal structure of *R. sphaeroides* CcO, which can be found in the database of Protein Data Bank (release no. 1M56), was used to generate this figure.

oxidase, samples were mixed with 2 mM prereduced cytochrome *c*. Both the CcO and cytochrome c^{2+} samples were degassed and saturated with $^{17}O_2$ at room temperature. The cytochrome c^{2+} and the CcO were mixed in the rapid freeze–quench (RFQ) apparatus, allowing several turnovers, and frozen by being sprayed into chilled isopentane maintained at 140 K. An incubation time before freezing of 4 msec, with the freezing process taking ≈5 msec, gives an overall reaction time of <10 msec. Starting CcO concentrations of ≈100 μM resulted in an ≈30 μM final concentration of CcO, after mixing, freezing, and packing into the EPR tube.

Paramagnetic Resonance Spectroscopy. Two- and three-pulse ESEEM spectra were recorded at 1.8 K by using a liquid helium immersion dewar under reduced [≈10 millibar (1 millibar = 100 PA)] pressure, on a pulsed EPR spectrometer constructed at Michigan State University (22). Processing of experimental ESEEM data and Fourier transformations was performed with MATLAB software from Mathworks (Natick, MA). Dead-time reconstruction (23), spectra normalization, and peak isolation (18) were performed as described. Continuous-wave X-band EPR spectra were measured on a Bruker (Billerica, MA) ESP300E equipped with either a TE112 or TE102 cavity resonator. Temperature was maintained at 10 K by using an Oxford ESR900 helium cryostat. All spectra were measured by using 2.0 mW of microwave power and a modulation amplitude of 8 G.

$H_2{}^{17}O$ with a ^{17}O enrichment of 48% was obtained from the Stable Isotope Resource at Los Alamos National Laboratory

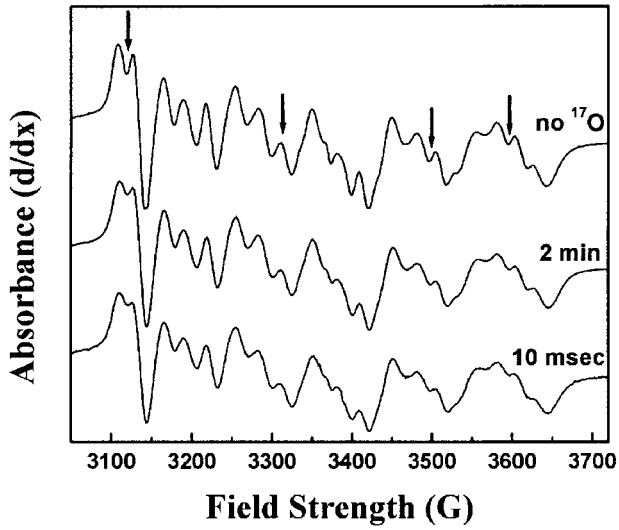

Fig. 3. Line-broadening of the Mn^{2+} spectrum after mixing with $H_2{}^{17}O$. The broadening of the Mn^{2+} pattern by interaction of the 5/2 nuclear spin of ^{17}O can be seen in samples incubated in 22% labeled $H_2{}^{17}O$ for several minutes (middle trace) and after 10 msec of incubation in 24% $H_2{}^{17}O$ (bottom trace). The broadening effects compared with the sample with no enrichment of ^{17}O (top trace) can best be seen where indicated by arrows. The clearest regions of line-broadening are marked by black arrows and are evidenced by the filling in of the peaks. The spectra were recorded at 10 K with a resonance frequency of 9.471 GHz by using the TE102 cavity. Each trace is an average of 20 scans.

(Los Alamos, NM). $^{17}O_2$ with an isotopic purity of 80% was from Isotec. Lauryl maltoside was Anagrade from Anatrace (Maumee, OH). All other chemicals were from Sigma.

Results

Exchange of Bulk Water. The ability of bulk water to access the Mg^{2+}/Mn^{2+} site on a catalytically relevant time scale was tested by mixing CcO with isotopically labeled water (24% final enrichment in ^{17}O) by using the RFQ system. The presence of isotopically labeled water, $H_2{}^{17}O$, at the Mg^{2+}/Mn^{2+} site could be assayed by line-broadening of the Mn^{2+} EPR spectrum. By using samples without ^{17}O as a reference, line-broadening (as evidenced by loss of resolution of the hyperfine structure) was detected to an equivalent extent in samples that had been incubated with labeled water for several minutes and RFQ samples that had been incubated for only 10 msec (Fig. 3). Additional evidence of ^{17}O presence near the Mn^{2+} could be seen by ESEEM, which shows a peak at the Larmour frequency of ^{17}O (Fig. 4). Although exact quantitation is difficult, the exchange appears to be completed within the fastest time of 10 msec, because no further broadening was observed after several minutes of incubation. This has also been observed for deuterium exchange (18).

Product Water Exit. Evidence for product water interacting with the Mn^{2+} was obtained by RFQ–EPR studies where catalytic turnover of the enzyme was initiated in the presence of 80% enriched $^{17}O_2$ substrate. The top trace of Fig. 5 shows the Mn^{2+} EPR spectrum that results from mixing $^{17}O_2$-saturated CcO with $^{17}O_2$-saturated buffer and is identical to the control spectrum of Fig. 3 (top trace). However, if $^{17}O_2$-saturated CcO samples are mixed with $^{17}O_2$-saturated reduced cytochrome *c* by using the RFQ system and allowed to turn over for 10 msec before freezing, significant broadening of the Mn^{2+} EPR spectrum is clearly observed (Fig. 5, second trace). Broadening is no longer seen to any significant extent when samples are allowed to complete five turnovers in ≈30 sec (Fig. 5, third trace), indicating

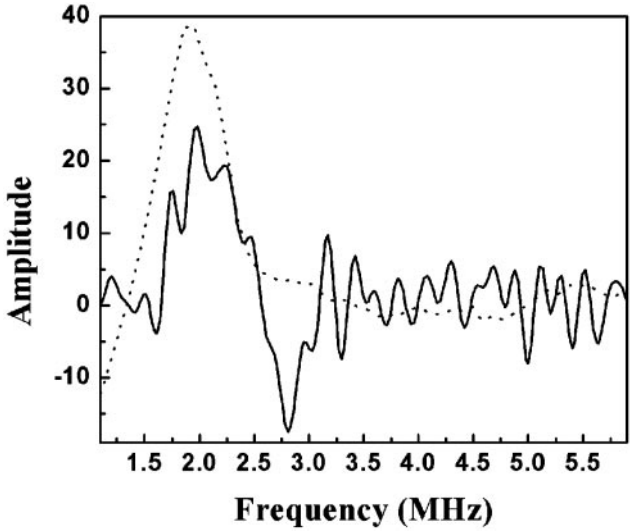

Fig. 4. ESEEM detection of a ^{17}O matrix line. Three-pulse ESEEM data from CcO incubated with 24% $H_2{}^{17}O$ for 10 msec (solid line) shows a peak at 2.2 MHz, the Larmour frequency of matrix ^{17}O at this field. $Mn^{2+}(H_2O)_6$ in 22% ^{17}O-enriched water (dotted line) also shows a peak at the same frequency. The large amount of noise in the CcO spectrum is caused by the small sample size and low concentration. Experimental conditions were as follows: temperature, 2 K; field strength, 3,420 G; microwave frequency, 8.852 GHz; power, 38 dBm; τ, 280 nsec; T, 40 nsec with 10-nsec increments.

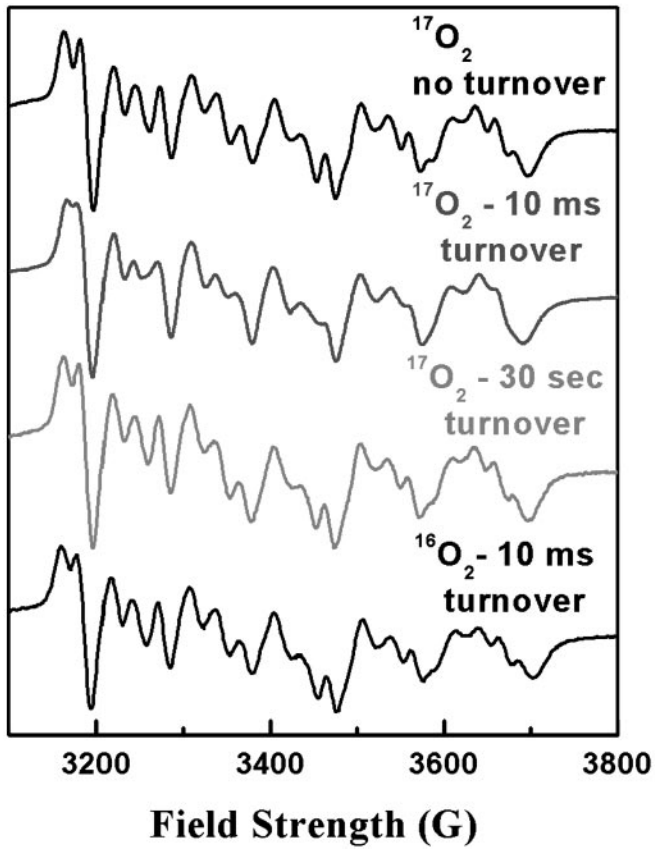

Fig. 5. Line-broadening of Mn^{2+} spectrum after turnover with $^{17}O_2$. The Mn^{2+} spectrum of CcO incubated with 80% enriched $^{17}O_2$ (top trace) shows no broadening, indicating no $^{17}O_2$ is bound at the metal. After 10 msec, which allows for fewer than five turnovers (second trace), severe line-broadening can be seen in all of the fine structure of the spectrum. This broadening was no longer seen after 30 sec of incubation (third trace), indicating that turnover had completed and the product water had escaped by this time. The spectrum of CcO saturated with $^{16}O_2$ and allowed to turn over for 10 msec (bottom trace) demonstrates that the broadening in the samples incubated in $^{17}O_2$ arises from product $H_2{}^{17}O$, not from the reduction of any of the metal cofactors. Experimental conditions are the same as in Fig. 3, except that the resonator used was the TE112 cavity with a resonance frequency of 9.623 GHz.

that the water produced at the active site has exchange with the bulk phase in this amount of time. To ensure that the line-broadening observed at 10 msec does not arise from the reduction of Cu_A, a sample saturated in $^{16}O_2$ was prepared in a similar fashion. Although a small amount of line-broadening was observed (Fig. 5, bottom trace), the level of broadening was not significant when compared with the $^{17}O_2$-turnover sample under our 10-msec turnover condition.

Discussion

The routes for proton uptake in CcO are relatively well defined, but there is little evidence regarding the proton/water release pathway(s). Previous work has shown that the buried Mn^{2+} site is accessible to proton or water exchange on a catalytically relevant time scale (18). However, because these studies were done with ^2H_2O, it could not be stated whether the observed exchange was of the entire water molecule or only the protons/deuterons of those water molecules. For further clarification of this issue, the same experiments were carried out with $H_2{}^{17}O$. A previous study had indicated that the Mn^{2+} in CcO was accessible to $H_2{}^{17}O$ after many hours of incubation, but the study contained no kinetic data (24). In the present study, water exchange was demonstrated by a ^{17}O matrix line in the ESEEM (Fig. 4) and line-broadening in the continuous wave-EPR spectrum (Fig. 3) on a catalytically relevant time scale.

Although these experiments validate the idea that a water exit path could involve Mn^{2+}, they do not necessarily imply that this pathway is actually used during catalysis or that it is unique. To test the actual use of the proposed channel during turnover, RFQ was used to look for isotopically labeled product water at the Mn^{2+} after turnover in $^{17}O_2$. If the $^{17}O_2$, converted to $H_2{}^{17}O$ at the active site, reaches the Mn^{2+}, it should broaden the continuous-wave EPR line shape. Surprisingly, major broadening of the Mn^{2+} spectrum was observed (Fig. 5), indicating that several water molecules bound to the metal (25, 26).

It was initially puzzling that a substantial amount of product $H_2{}^{17}O$ was observed at the Mn^{2+}, because it seems to contradict our previous results showing rapid exchange of water with the bulk phase in the same time frame (<10 ms) (18). However, calculations extrapolated from the number of turnovers completed in 10 msec as measured by cytochrome *c* oxidation in stopped-flow experiments indicate that the turnover of the enzyme would continue until the sample was actually frozen. By using a CcO concentration of $\approx$50 μM and an O_2 concentration of 1 mM (saturated at room temperature) and by providing electrons as reduced cytochrome *c* at $\approx$1 mM, the reaction was limited by reducing equivalents to five or fewer complete conversions of O_2 to two H_2O molecules per CcO molecule (four electrons are required to convert one $^{17}O_2$ molecule to two $H_2{}^{17}O$ molecules). Even if all of the cytochrome c^{2+} is oxidized, no more than 10 water molecules can be produced per CcO during the reaction time. In fact, under the conditions of this experiment, 10 is an upper limit for $H_2{}^{17}O$ production, because the increasing levels of oxidized cytochrome *c* compete with reduced cytochrome *c*, causing the rate of turnover to slow down exponentially as the reaction proceeds. Previous stopped-flow kinetic studies, when similarly limited by substrate electrons, suggest that only approximately two complete turnovers would occur within the first 10 msec of the reaction (27), producing an average of four to six water molecules per CcO and resulting in

continued availability of reducing equivalents until the end of the 10 msec before freezing.

Because of the large discrepancy in the amount of labeled water produced at the active site, giving a maximum of 1 mM labeled water, as compared to the concentration of water in the bulk (55,000:1 ratio), any labeled water that reached the bulk phase would be so diluted that diffusion back into the Mg^{2+}/Mn^{2+} site would be negligible. This finding is validated by the lack of line-broadening seen in samples saturated in $^{17}O_2$ that have been incubated with reduced cytochrome *c* for 30 sec, which is enough time to allow for the completion of turnover and exchange of the produced water with the bulk. Hence, any labeled water coupled to the Mn^{2+} must have come directly from the active site. Given the level of broadening and the limited number of product water molecules produced, it is likely that most or all of the water molecules exit by means of this route. Thus, the appearance of water at the Mg^{2+}/Mn^{2+} site in only a few turnovers argues strongly against the idea that water exits by random diffusion from the active site of CcO. The large degree of line broadening produced is convincing evidence that this is not just one of several specific exit routes for water (13, 28) but likely the exclusive route used for water exit. Were water exit to occur in either a simultaneous or alternating fashion along other routes that do not pass the Mg^{2+}/Mn^{2+} site (such as the proposed exit through the oxygen channel; see ref. 28), such dramatic line-broadening should not be observed. The significant line-broadening described here requires several product water molecules to be directly ligated to the Mn^{2+}.

There are several species that do not have the Mg^{2+} site in their CcO (20), which brings into question the necessity for this metal site in CcO function. However, its conservation in all eukaryotic CcO and several bacterial CcO suggests this site may have an important role. The exit of water from the active site to the positive external surface opens the possibility of proton back-leak from the outside to the active site, effectively short-circuiting the pump. The Mg^{2+}/Mn^{2+} could provide a mechanism for preventing this back-leak of protons by electrostatic repulsion, if the water exit/back-leak channel involves ligation to the metal. Forms of CcO that do not have a metal at this site may have a different proton exit pathway and/or a less well controlled activity (29). No proton exit channel has been clearly defined in the limited number of species for which the crystal structure of CcO has been determined, so there is not enough evidence to indicate whether the proton exit pathway is strictly conserved across different species.

The results described define a major water exit pathway that reaches the Mg^{2+}/Mn^{2+} from the heme a_3–Cu_B site. From there, it has rapid access to the bulk phase, but the exact pathway from Mg^{2+} to the outside has not been defined. It is conceivable that there is no defined pathway through the remaining, more hydrophilic region of the protein. It is also conceivable that the water pathway is involved in proton transfer as well. The technology that we have established will allow us to address these questions.

We thank Dr. Joan Broderick for the extensive use of her RFQ apparatus. This work was supported by National Institutes of Health Grants GM26196 (to S.F.M.), P01-GM 57323 (to S.F.M and J.M.), and RR02231 (to the National Stable Isotope Resource at Los Alamos).

1. Ferguson-Miller, S. & Babcock, G. (1996) *Chem. Rev. (Washington, D.C.)* **96,** 2889–2907.
2. Wikström, M. (1977) *Nature* **266,** 271–273.
3. Fetter, J. R., Qian, J., Shapleigh, J., Thomas, J. W., García-Horsman, J. A., Schmidt, E., Hosler, J., Babcock, G. T., Gennis, R. B. & Ferguson-Miller, S. (1995) *Proc. Natl. Acad. Sci. USA* **92,** 1604–1608.
4. Iwata, S., Ostermeier, C., Ludwig, B. & Michel, H. (1995) *Nature* **376,** 660–669.
5. Tsukihara, T., Aoyama, H., Yamashita, E., Tomizaki, T., Yamaguchi, H., Shinzawa-Itoh, K., Nakashima, R., Yaono, R. & Yoshikawa, S. (1995) *Science* **269,** 1069–1074.
6. Puustinen, A. & Wikström, M. (1999) *Proc. Natl. Acad. Sci. USA* **96,** 35–37.
7. Mills, D. A., Florens, L., Hiser, C., Qian, J. & Ferguson-Miller, S. (2000) *Biochim. Biophys. Acta* **1458,** 180–187.
8. Michel, H. (1998) *Proc. Natl. Acad. Sci. USA* **95,** 12819–12824.
9. Mills, D. A. & Ferguson-Miller, S. (1998) *Biochim. Biophys. Acta* **1365,** 46–52.
10. Florens, L., Hoganson, C., McCracken, J., Fetter, J., Mills, D. A., Babcock, G. T. & Ferguson-Miller, S. (1999) in *The Phototropic Prokaryotes*, eds. Peschek, G., Löffelhard, W. & Schmetterer, G. (Kluwer–Plenum, New York), pp. 329–339.
11. Tsukihara, T., Aoyama, H., Yamashita, E., Tomizaki, T., Yamaguchi, H., Shinzawa-Itoh, K., Nakashima, R., Yaono, R. & Yoshikawa, S. (1996) *Science* **272,** 1136–1144.
12. Soulimane, T., Buse, G., Bourenkov, G. P., Bartunik, H. D., Huber, R. & Than, M. E. (2000) *EMBO J.* **19,** 1766–1776.
13. Backgren, C., Hummer, G., Wikström, M. & Puustinen, A. (2000) *Biochemistry* **39,** 7863–7867.
14. Garcia, A. E. & Hummer, G. (2000) *Proteins* **38,** 261–272.
15. Gottschalk, M., Dencher, N. A. & Halle, B. (2001) *J. Mol. Biol.* **311,** 605–621.
16. Nagle, J. F. & Morowitz, H. J. (1978) *Proc. Natl. Acad. Sci. USA* **75,** 298–302.
17. Pomes, R. & Roux, B. (1998) *Biophys. J.* **75,** 33–40.
18. Florens, L., Schmidt, B., McCracken, J. & Ferguson-Miller, S. (2001) *Biochemistry* **40,** 7491–7497.
19. Zhen, Y., Qian, J., Follmann, K., Hosler, J., Hayward, T., Nilsson, T. & Ferguson-Miller, S. (1998) *Protein Expression Purif.* **13,** 326–336.
20. Hosler, J. P., Espe, M. P., Zhen, Y., Babcock, G. T. & Ferguson-Miller, S. (1995) *Biochemistry* **34,** 7586–7592.
21. Mitchell, D. M. & Gennis, R. B. (1995) *FEBS Lett.* **368,** 148–150.
22. McCracken, J., Shin, D.-H. & Dye, J. L. (1992) *Appl. Magn. Reson.* **3,** 305–316.
23. Mims, W. B. (1984) *J. Magn. Reson.* **59,** 291–306.
24. Haltia, T. (1992) *Biochim. Biophys. Acta* **1098,** 343–350.
25. Kofron, J. L., Ash, D. E. & Reed, G. H. (1988) *Biochemistry* **27,** 4781–4787.
26. Bellew, B. F., Halkides, C. J., Gerfen, G. J., Griffin, R. G. & Singel, D. J. (1996) *Biochemistry* **35,** 12186–12193.
27. Zhen, Y., Mills, D., Hoganson, C. W., Lucas, R. L., Shi, W., Babcock, G. & Ferguson-Miller, S. (1999) in *Frontiers of Cellular Bioenergetics: Molecular Biology, Biochemistry and Physiopathology*, eds. Papa, S., Guerrieri, F. & Tager, J. M. (Kluwer–Plenum, New York), pp. 157–178.
28. Zheng, X., Medvedev, D. M., Swanson, J. & Stuchebrukhov, A. A. (2003) *Biochim. Biophys. Acta* **1557,** 99–107.
29. Mills, D. A. & Ferguson-Miller, S. (2002) *Biochim. Biophys. Acta* **1555,** 96–100.